Selfaligned InGaAs/GaAs/InGaP quantum well lasers prepared by gassource molecular beam epitaxy with two growth steps

Y. K. Chen, M. C. Wu, J. M. Kuo, M. A. Chin, and A. M. Sergent

Citation: Applied Physics Letters **59**, 2929 (1991); doi: 10.1063/1.105854
View online: http://dx.doi.org/10.1063/1.105854
View Table of Contents: http://scitation.aip.org/content/aip/journal/apl/59/23?ver=pdfcov
Published by the AIP Publishing

Self-aligned InGaAs/GaAs/InGaP quantum well lasers prepared by gas-source molecular beam epitaxy with two growth steps

Y. K. Chen, M. C. Wu, J. M. Kuo, M. A. Chin, and A. M. Sergent
AT&T Bell Laboratories, 600 Mountain Avenue, New Jersey 07974

(Received 7 August 1991; accepted for publication 21 September 1991)

Index-guided self-aligned InGaAs/GaAs/InGaP quantum well lasers are fabricated by gas-source molecular beam epitaxy in two growth sequences on a GaAs substrate for the first time. The use of aluminum-free InGaP as cladding layers permits regrowth steps without the problem with the oxidation of aluminum alloys. A patterned *n*-InGaP current confinement layer is used to provide index guiding as well as current blocking. Preliminary results from coated 2.5-μm-wide and 508-μm-long devices show a room temperature continuous wave lasing threshold current of 12 mA with an external differential quantum efficiency of 0.68 mW/mA and a characteristic temperature of 130 K from 30 to 75 °C.

Strained-layer InGaAs semiconductor quantum well lasers are very important for many applications such as sources for optical data storage and optical pumps for the doped glass lasers and amplifiers. In particular, high power quantum well lasers with 980 nm emission wavelength are very desirable to pump high efficiency and low noise erbium-doped fiber amplifiers for the ultralong distance transmission of 1.55 μm optical signals in the lowest loss transmission band of silica fibers.[1] More recently, praseodymium (Pr)-based fluoride fiber also show very high gain ($\sim$38 dB) for amplifying optical signals in the 1.3 μm transmission band.[2] The optimal pump wavelength for the Pr-doped fiber is around 1.01 μm, which can also be provided by the strained-layer InGaAs quantum well lasers. Most of the strained-layer InGaAs lasers reported to date used AlGaAs as cladding layers.[3–5] Because of the problem with the removal of the stable oxide on the regrowth surface of aluminum alloy, it is difficult to fabricate high performance index-guided laser structures such as buried heterostructure lasers. Low aluminum composition of the cladding layers was used for the ease of regrowth.[6] However, its carrier confinement may not be sufficient under high injection conditions or high temperature operations. High aluminum composition is particularly difficult for laser structures using molecular beam epitaxy (MBE) with multiple regrowth steps, where the stable oxide on the AlGaAs layer cannot be easily removed with the common techniques such as melt back in liquid phase epitaxy (LPE) regrowth[7] or *in situ* vapor etching in organometallic vapor phase epitaxial (OMVPE) regrowth.[8] Previously, *in situ* selective thermal etching of a thin GaAs oxidation-prevention layer before the MBE regrowth was used to fabricate single mode self-aligned AlGaAs double heterostructure lasers.[9] However, only the narrow band gap GaAs confining layer can be patterned for the *in situ* thermal etching, which limits many applications requiring patterned layers with large energy band gap.

Recently, the $In_{0.49}Ga_{0.51}P$ layer (this will be briefed as InGaP throughout the text) lattice matched to the GaAs substrate has generated a lot of interests because it can be used as an alternative wide band-gap material to substitute the widely used AlGaAs alloys for electronic and optical devices. The high etching selectivity between InGaP and GaAs simplifies processing and promises tight control. Electron mobility[10] as high as 780,000 cm^2/V s and interface recombination velocity[11] as low as 1.5 cm/s were reported for GaAs–InGaP heterostructures. Strained-layer InGaAs quantum well lasers with lattice-matched InGaP cladding layers have been reported with low threshold current density[12] (72 A/cm^2) and high operation temperature[13] (185 °C), which are comparable to the best reported performance of strained-layer AlGaAs lasers.[3,14] Index-guided laser structures such as ridge waveguide[12,13] and buried heterostructure with mass transport[15] of InGaP were also demonstrated successfully. However, the MBE regrowth on the aluminum-free InGaP surface has not been exploited yet. In this letter, we report on the first successful fabrication of index-guided self-aligned InGaAs/GaAs/InGaP quantum well lasers by gas source molecular-beam epitaxy (GSMBE) in two growth steps. A patterned *n*-doped InGaP confining layer together with a regrown GaAs wave guiding layer provide the current blocking and index guiding in a large optical cavity (LOC) configuration. The coated 2.5-μm-wide, 508-μm-long laser shows a continuous wave (cw) lasing threshold current of 12 mA and an external quantum efficiency of 0.68 mW/mA. It lases in a single longitudinal mode at $\sim$1 μm emission wavelength. Peak optical power up to 83 mW is obtained from a 4.5-μm-wide, 508-μm-long laser before catastrophic optical damage (COD) at facets.

The layer structure of the self-aligned $In_{0.2}Ga_{0.8}As/GaAs/In_{0.49}Ga_{0.51}P$ quantum well laser is shown in Fig. 1. This structure is grown on n^+-GaAs substrate by GSMBE in two growth sequences. Detailed growth parameters and conditions are similar to those of the InGaAs/GaAs/InGaP broad area lasers reported in Ref. 16. The first growth sequence consisted of ten pairs of n^+-doped InGaP/GaAs superlattice as the buffer layer, a 1.5-μm-thick n^+-InGaP cladding layer, a 1000-Å-thick GaAs separate confinement heterostructure (SCH) layer, three $In_{0.2}Ga_{0.8}As$/GaAs (70 Å/200 Å) strained quantum wells as the active medium, a 1000-Å-thick GaAs SCH

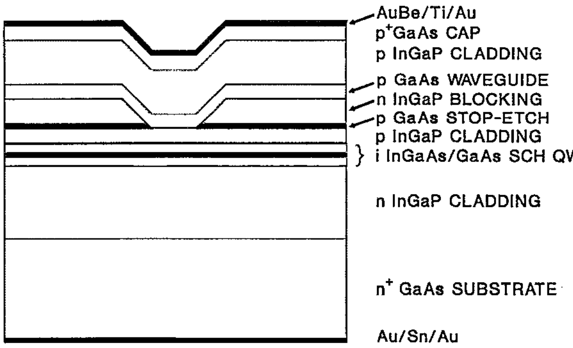

FIG. 1. Schematic diagram shows the layer structure of self-aligned $In_{0.2}Ga_{0.8}As/GaAs/In_{0.49}Ga_{0.51}P$ multiple quantum well structure using two-step growth with the gas source molecular beam epitaxy (GSMBE). A patterned n-doped InGaP is used as the blocking and confinement layer with the aluminum-free regrowth surface.

layer, a 1000-Å thick p^+-InGaP barrier layer, a 100-Å-thick p^+-GaAs stop-etch layer, and a 2000-Å-thick n^+-InGaP blocking layer. After the first growth, the wafer was patterned with SiO_2 window stripes of various widths. The stripes were aligned along the $\langle 1\bar{1}0\rangle$ crystal orientation to provide etching profiles with positive slopes. Channels of 2.5 and 4.5 μm width were delineated by removing the exposed n^+-InGaP blocking layer with selective wet chemical etching. After removing the SiO_2 etch mask and the exposed thin p^+-GaAs stop-etch layer, the wafer was loaded into the chamber for the second growth sequence. The all-InGaP surface is important for regrowth to avoid potential problems of the exposed GaAs surface, which is unstable in the phosphorus flux[15] during the initial *in situ* high temperature removal of surface oxide. During the second growth, the following layers were grown: a 1000-Å-thick p^+-GaAs waveguide layer, a 1.0-μm-thick p^+-InGaP cladding layer, and a 2000-Å-thick p^+-GaAs cap layer.

Previously, most of the self-aligned laser structures utilized a patterned low band gap (or high refractive index) GaAs layer for current blocking and guiding of the lateral mode.[9,17,18] The lateral mode in these structures is stabilized by the loss as well as the refractive index difference from the embedded anti-guiding small band gap confining layer.[17] In our structure, the patterned wide band gap n^+-InGaP layer is reverse biased as the current confinement layers. It also provides lateral optical confinement to the first regrown GaAs waveguide layer. To guide the lateral mode, the regrown high-index p^+-GaAs waveguide layer, which fills in the opening of the low-index n^+-InGaP blocking layer, couples the optical field from the active medium to constitute a large optical cavity and provides the necessary index guiding. After the second growth sequence, the wafer was thinned down to 4 mils and alloyed with AuBe/Ti/Au and Au/Sn/Au as p- and n-type metal contact layers, respectively. Then the laser stripes were cleaved and mounted with the junction side up on copper heat sinks for evaluations.

Figure 2 shows the continuous wave (cw) light-current (L–I) characteristics of antireflection (AR)/high-reflection (HR) coated self-aligned lasers at room temperature. The facet reflectivities are ~0.1 and 0.91 for the AR- and HR-coated facets, respectively. Threshold currents of 12 and 14 mA are achieved for the 508-μm-long lasers with 2.5- and 4.5-μm-wide openings, respectively. In the absence of the lateral carrier confinements in the active region, the current spreading is high in these lasers (~8 mA), as estimated from the dependence of threshold current on channel width from 2.5 to 12 μm. The external differential quantum efficiency is 0.68 mW/mA at room temperature. The peak power emitted into free space from these AR/HR-coated lasers is 61 mW for the 2.5-μm-wide laser and 83 mW for the 4.5-μm-wide laser. The inset in Fig. 2 shows the far field radiation pattern of the 2.5-μm-wide laser. A full width at half-maximum (FWHM) angle of 54° is obtained in the transverse direction ($\theta_\perp$, perpen-

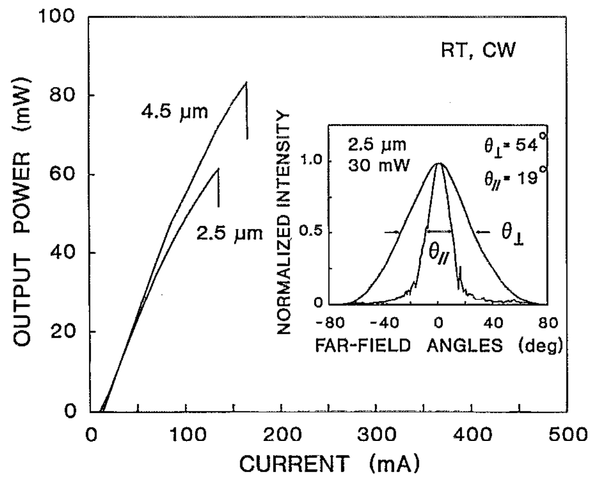

FIG. 2. The continuous wave (cw) light-current characteristics of coated self-align lasers with 508-μm-long cavity at room temperature. The channel widths are 2.5 and 4.5 μm wide, respectively. The inset shows the far filed radiation pattern of a 2.5-μm-wide laser with $\theta_\perp = 54°$ and $\theta_\| = 19°$.

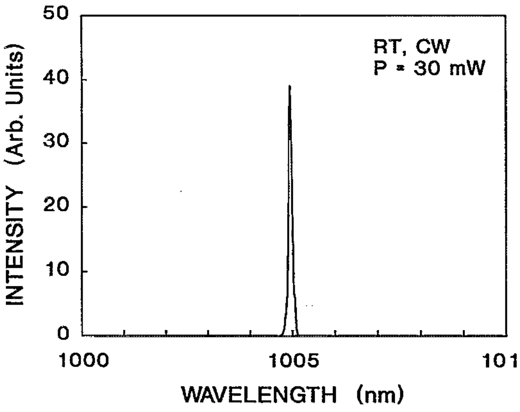

FIG. 3. The lasing spectrum of a 2.5 μm×508 μm laser at 30 mW cw output power. It shows a single mode emission at 1.005 μm with a side-mode suppression ratio greater than 30 dB.

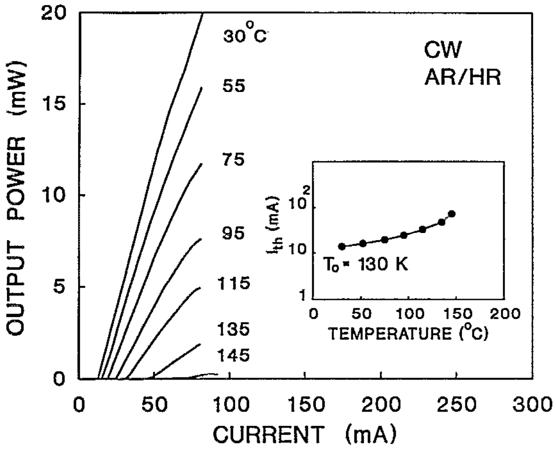

FIG. 4. The temperature dependence of the L–I characteristics of a 2.5 μm×508 μm AR/HR-coated laser from 30 to 145 °C. The insert shows the threshold current vs temperature. A characteristic temperature (T_0) of 130 K is obtained from 30 to 75 °C.

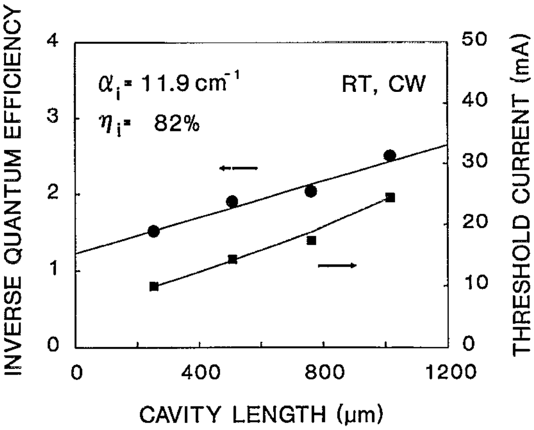

FIG. 5. The cavity length dependence of the cw threshold current and the reciprocal external differential efficiency of uncoated 2.5-μm-wide self-aligned lasers. It shows an internal differential quantum efficiency (η_i) of 82% and a waveguide loss (α_i) of 11.9 cm^{-1} at room temperature.

dicular to the junction plane) and 19° in the lateral direction ($\theta_{\parallel}$). The peak power is limited by the tightly confined optical modes in the cavity and can be increased significantly by using the much expanded cavity design such as the periodic index separate confinement heterostructure (PINSCH) lasers.[19] The lasing spectrum of a 2.5×508 μm laser is shown in Fig. 3. It shows a single mode emission spectrum centered at 1005 nm at 30 mW output power with a side-mode suppression ratio more than 30 dB. This emission wavelength locates in the pump band of the Pr-doped fiber reported in Ref. 2. Fundamental mode lasing is observed up to the highest power for this 2.5-μm wide laser. This demonstrates the effectiveness of the index guiding in this self-aligned structure.

The temperature dependent L–I curves of the AR/HR-coated laser are plotted in Fig. 4 from 30 to 145 °C. The inset of Fig. 4 shows the temperature dependence of the threshold current. By fitting the threshold current to $I_{th} = I_0 \exp(T/T_0)$, the characteristic temperature (T_0) is 130 K, where T is the temperature and I_0 is the extrapolated threshold current at low temperature ($T = 0$ °C). From the L–I curves of 2.5-μm wide uncoated lasers of various cavity lengths, the room-temperature cw internal differential quantum efficiency (η_i) is estimated to be 82% with a waveguide loss (α_i) of 11.9 cm^{-1}, as shown in Fig. 5.

In summary, the aluminum-free InGaP layers lattice-matched on the GaAs substrate have been utilized to fabricate self-aligned index-guided InGaAs/GaAs/InGaP lasers by gas source molecular-beam epitaxy (GSMBE) in two growth sequences. Very low threshold current (12 mA), high temperature operation (up to 145 °C), and fundamental mode radiation pattern have been achieved with AR/HR-coated 2.5 μm×508 μm lasers. This work demonstrates the regrowth capability of the gas source MBE technique to fabricate high performance optoelectronic circuits (OEICs) and devices on the patterned aluminum-free InGaP layers.

[1] R. I. Laming, M. C. Farries, P. R. Morkel, L. Reekie, and D. N. Payne, Electron. Lett. **25**, 12 (1989).
[2] Y. Miyajima, T. Sugawa, and Y. Fukasaku, IEEE Topical Meeting on Optical Amplifiers, Post-deadline paper, PD1, Snowmass, Colorado, 1991 (unpublished).
[3] H. K. Choi and C. A. Wang, Appl. Phys. Lett. **57**, 321 (1990).
[4] M. Okayasu, T. Takeshita, M. Yamada, O. Kogure, N. Horiguchi, M. Fukuda, A. Kozen, K. Oe, and S. Uehara, Electron. Lett. **25**, 1563 (1989).
[5] D. Bour, N. Dinkel, IEEE Photon Technol. Lett. **2**, 153 (1990).
[6] P. K. York, K. J. Beernink, G. E. Fernandez, and J. J. Coleman, Appl. Phys. Lett. **54**, 499 (1989).
[7] T. R. Chen, L. E. Eng, Y. H. Zhuang, Y. J. Xu, H. Zaren, and A. Yariv, Appl. Phys. Lett. **57**, 2762 (1990).
[8] M. Nido, I. Komazaki, K. Kobayashi, K. Endo, M. Ueno, T. Kamejima, and T. Suzuki, IEEE J. Quantum Electron. **QE-23**, 720 (1987).
[9] H. Tanaka, M. Mushiage, Y. Ishida, and H. Fukada, Jpn. J. Appl. Phys. **24**, L89 (1985).
[10] M. Razeghi, M. Defour, F. Omnes, M. Dobers, J. P. Vieren, and Y. Guldner, Appl. Phys. Lett. **55**, 457 (1989).
[11] J. M. Olson, R. K. Ahrenkiel, D. J. Dunlavy, B. Keyes, and A. E. Kibbler, Appl. Phys. Lett. **55**, 1208 (1989).
[12] T. Ijichi, M. Ohkubo, N. Matsumoto, and H. Okamoto, Tech. Digest of IEEE 12th International Semiconductor Laser Conference 1990, Davos, Swiss (unpublished), p. 44.
[13] M. C. Wu, Y. K. Chen, J. M. Kuo, M. A. Chin, and A. M. Sergent (unpublished).
[14] R. J. Fu, C. S. Hong, E. Y. Chan, D. J. Booher, and L. Figueroa, IEEE Photon. Technol. Lett. **3**, 308 (1991).
[15] S. H. Groves, Z. L. Liau, S. C. Palmateer, and J. N. Walpole, Appl. Phys. Lett. **56**, 312 (1990).
[16] J. M. Kuo, Y. K. Chen, M. C. Wu, and M. A. Chin, Appl. Phys. Lett. **59**, 2781 (1991).
[17] M. Yano, H. Nishi, and M. Takusagawa, IEEE J. Quantum. Electron. **QE-15**, 1388 (1979).
[18] J. J. Coleman and P. D. Dapkus, Appl. Phys. Lett. **37**, 262 (1980).
[19] M. C. Wu, Y. K. Chen, M. H. Hong, J. P. Mannaerts, and M. A. Chin, Appl. Phys. Lett. **59**, 1046 (1991).